PAPER • **OPEN ACCESS**

Microstructure evolution in an Al-Si piston alloy under ultrasonic melt processing

To cite this article: Suwaree Chankitmunkong *et al* 2019 *IOP Conf. Ser.: Mater. Sci. Eng.* **529** 012060

View the article online for updates and enhancements.

IOP ebooks™

Bringing you innovative digital publishing with leading voices to create your essential collection of books in STEM research.

Start exploring the collection - download the first chapter of every title for free.

This content was downloaded from IP address 117.95.192.164 on 18/09/2019 at 19:14

IOP Conf. Series: Materials Science and Engineering **529** (2019) 012060 doi:10.1088/1757-899X/529/1/012060

Microstructure evolution in an Al-Si piston alloy under ultrasonic melt processing

Suwaree Chankitmunkong[1, 2*], Dmitry G. Eskin[2, 3], and Chaowalit Limmaneevichitr[1]

[1]Department of Production Engineering, Faculty of Engineering, King Mongkut's University of Technology Thonburi, 126 Pracha-Utid Rd., Bangmod, Tungkhru, Bangkok, 10140 Thailand
[2]Brunel University London, BCAST, Uxbridge, Middlesex UB8 3PH, United Kingdom
[3]Tomsk State University, Tomsk 634050, Russian Federation

*suwaree.03@mail.kmutt.ac.th

Abstract. Piston Al-Si eutectic alloys are used to produce direct-chill cast billets for subsequent forging. Because of a very complex composition and multi-phase heterogeneous structure, it is necessary to control the formation of primary and eutectic compounds either through alloying or casting conditions (or both). In this study we used ultrasonic melt processing above or across the liquidus line to affect the occurrence and size distribution of primary Si as well as morphology of primary Al dendrites and high-temperature eutectic phases. The refinement of these particles has potential benefit for mechanical properties and formability during forging.

1. Introduction

Al-Si piston alloys have been widely used in automotive industry due to their high strength, excellent castability, good wear resistance and low thermal expansion. These alloys are also used to produce hot forged engine parts. Generally, the mechanical properties of an Al-Si piston alloy are dominated by the complex microstructure with primary and eutectic phases such as α-Al, primary and eutectic Si, Mg_2Si, Al_2Cu, $Al_5Cu_2Mg_8Si_6$, Al_3Ni, Al_3CuNi and Al_7Cu_4Ni phases. Moreover, the addition of Cu and Mg is also used to improve the mechanical properties of Al-Si piston alloys through heat treatment [1, 2]. The amount, size and morphology of primary silicon and primary Al dendrites play role in the deformation process and affect the mechanical properties of final products. Furthermore, the β-phase ($Al_9Fe_2Si_2$) intermetallic is considered as a harmful phase in Al-Si alloys, particularly the large size and elongated morphology of this phase play detrimental role in mechanical properties [3]. Thus, it is important to refine or modify the hard particles such as primary Si and β-phase intermetallics, as well as achieve a uniformly equiaxed grain structure of primary aluminium in a billet. Generally, the addition of alloying elements to aluminium is a conventional method used to modify the microstructure. Ultrasonic melt treatment (UST) is shown to be efficient in refining grains, primary particles and small intermetallics [4]. However, the mechanisms and effects of UST relate to the temperature ranges in which it is applied to the melt [5, 6].

The purpose of this work is to study the microstructural evolution of an Al-Si piston alloy with high Cu content upon ultrasonic treatment during solidification, and relate the observed effects to the mechanisms of ultrasonic treatment, for improving the microstructure and hardness.

2. Material and methods

The experimental alloys were prepared using high-purity Al (99.9 wt%), commercial 99.5 wt% pure Mg and Al–45 wt% Si, Al–45 wt% Cu, Al–20 wt% Ni and Al–45 wt% Fe master alloys. The composition of the alloy was analysed by emission spectrometry and given in Table 1. This is essentially an AA4032 alloy with increased Cu concentration. The alloy was melted in a clay graphite crucible in an electric resistance furnace. The molten metal was maintained at 750 ± 5 °C. UST was performed with a 5-kW ultrasonic generator (Reltec) and a 5-kW water-cooled magnetostrictive transducer (Reltec) with a niobium sonotrode 20 mm in diameter at a working frequency of 17.5 kHz (amplitude ±20 μm). The experimental set up is designed to observe the effect of UST at different stages during solidification.

Content from this work may be used under the terms of the Creative Commons Attribution 3.0 licence. Any further distribution of this work must maintain attribution to the author(s) and the title of the work, journal citation and DOI.
Published under licence by IOP Publishing Ltd

The steel mould (Figure 1) was covered by insulation material from outside to minimize heat losses from the mould wall, while being placed on a massive steel base to assure the progressive solidification from the bottom to the top. The sonotrode preheated to 600 °C was located at the top part of the mould, so that it will be submerged into the liquid metal by approximately 5 mm when the mould is filled with the melt. The molten metal was poured at 720 °C. When the mould was completely filled, the ultrasonic transducer was turned on. Therefore, the solidifying metal at the bottom part of the sample was not affected by UST (No UST). As the solidification progressed from the bottom towards the sonotrode, the solidifying alloy experienced action of ultrasound at different stages of solidification: first in the liquid phase only, then (in the middle part of the mould) across the liquidus, and finally in the mushy zone in the upper part of a billet as can be seen in Figure 1.

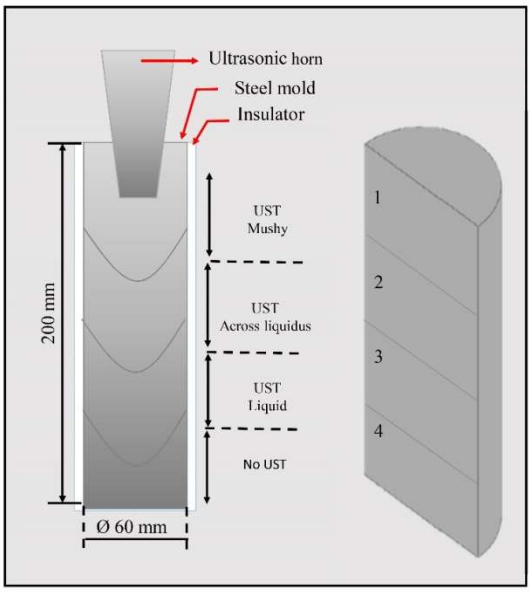

Figure 1. Schematic diagram of experimental set up of casting at different stages of ultrasonic treatment

Table 1. Chemical composition of Al-Si piston alloy with high Cu content as determined by emission spectrometry

Alloy	Chemical composition (wt.%)					
	Si	Cu	Mg	Ni	Fe	Al
3.5Cu	12.7	3.56	0.92	1.07	1.29	Balance

The microstructures were examined in vertical sections reflecting each stage of UST, from the mushy zone, across the liquidus, in liquid and without UST by standard metallographic procedures. The microstructure and intermetallics were observed by optical microscope (OM) and scanning electron microscope (SEM). Prior to observation, the samples were etched by Keller's reagent (5 ml HNO_3, 3 ml HCl and 2 ml HF in 190 ml distilled water) for 1 min. Polished samples were also anodized in Barker's solution (5% HBF4 water solution) for about 2 min at 20 VDC and were then examined under polarized light. The grain sizes were measured using the linear intercept method according to ASTM E112-10. The quantitative measurement of primary Si particles size and grain size were carried out using image analysis software. The iron-containing intermetallics were also analysed for the chemical composition in a ZEISS Supra 35 SEM with an energy dispersive spectroscopy (EDS). Hardness tests were conducted by a Brinell hardness testing machine with 187.5 N load, 2.5 mm ball indenter, and 20 s dwell time.

3. Results and discussion

3.1. Primary Si particles and α-Al dendrite transformation

To investigate the effect of UST treatment on the microstructure evolution at different stages of solidification, the macrostructure of the billet cross-sections was observed, and can be seen in Figure 2 (a-b). The results show that the grain macrostructure started to change when UST had been applied in the liquid stage, as compared to the bottom section of the billet where no UST had been felt and where the grain morphology was coarse. After the ultrasonic transducer was turned on and the solidification front moved upwards to the ultrasonic source, the macrostructure started to refine with a clear transition seen as the dashed line region in Figure 2c (the transition between UST and no UST treatment). This indicates that the UST was effective even when applied in the liquid state. As the solidification front was moving upwards, the grain size of Al dendrites progressively decreased, while the amount of primary Si increased, see Figure 2 (a-c, e-g).

The quantitative analysis of Al grains and primary Si is given in Figure 3. The smallest size of primary Si particles is about 35μm and is achieved when the alloy was treated with ultrasound in the liquid state, which is smaller than in the alloy treated by UST across the liquidus (42 μm), and in the mushy stage resulted in the size of primary Si particles become slightly increased. In all cases of UST the primary Si was significantly refined. However, the amount of primary Si particles is highest when UST was applied across the liquidus and in the mush, which also corresponded to a more homogenous distribution of these particles in the structure (Figure 2e, f). This is a desired effect as it makes the stress concentration on brittle particles less probably in the microstructure under load, and may improve the toughness of the alloy. The increased amount and simultaneous refinement of primary Si particles can be attributed to the effect of acoustic cavitation upon UST on the nucleation process of primary Si (when applied above and across the liquids) and fragmentation of these particles (when applied across and below the liquids). Similar effects have been observed upon UST for primary Si [5], Al_3Zr and Al_3Ti primary particles [7, 8]. Moreover, the UST treatment might also increase the melt temperature (by a few degrees) that later limit the growth of primary particles.

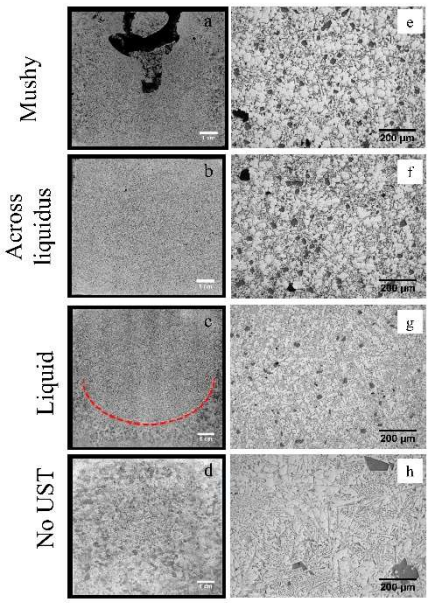

Figure 2. Macrostructure and microstructure of the Al-Si piston alloy with applied UST at different stages of solidification. (The red-dashed line depicts the beginning of UST effect)

Figure 3b also confirms that the grain size was progressively and significantly decreased as the solidification front was moving towards the sonotrode. Figure 4 (a-d) shows the effects of UST treatment

on the refinement and the growth morphology of Al grains. It is clear that the morphology of Al grains changed from coarse dendritic to tiny globular when UST was applied in the mushy stage as compared to the alloy without UST treatment (Figure 4a, d), which correlated to refinement of the grain from about 250 to 50 µm. The Al dendrites also became finer when the UST was applied in the liquid state and across the liquidus. In these cases one can observe a mixed structure with dendritic and globular grains. It is well known that the grain refinement is directly related to the number of active nuclei in the melt. Hence, when UST was applied at high temperature (liquid stage), the main mechanism should be related to the cavitation-induced heterogeneous nucleation, e.g. on oxides [4]. While when UST was applied at lower temperature (across and below the liquidus), in addition to the already effected heterogeneous nucleation, dendrite fragmentation caused by cavitation and acoustic flows resulted in grain multiplication and refinement [9]. This led to the most significant grain refinement achieved upon UST in the mushy stage.

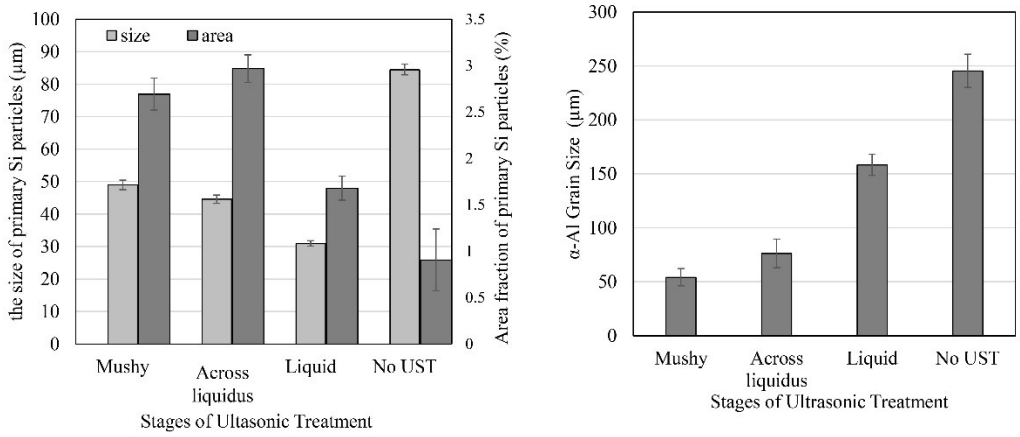

Figure 3. The quantitative analysis of the Al-Si piston alloy; (a) the size and amount of primary Si particles, (b) size of α-Al grains without and with UST applied at different stages of solidification.

3.2. Effect of UST on the morphology of Fe-containing intermetallic

Figure 5 shows SEM images of the microstructure with Fe-containing intermetallics without UST and with UST across the liquidus. The iron-containing intermetallic phases were quite large in the Al-Si piston alloy without UST, and can be clearly seen as elongated needle-like crystals in eutectic regions (Figure 5a, shown by red arrow). After UST the morphology of these phases changed to short rods as can be seen in Figure 5b (shown by red arrows). We assume that this change was due to the ultrasonic fragmentation mechanism similar to that observed in Ref.[10]. The chemical composition of Fe-containing intermetallics were measured by EDS spot analysis with averaging over seven measured particles, and the results are listed in Table 2. Although the chemical composition of the rod-like phase is slightly different from the needles-shaped particles, the compositional range reflect the β-$Al_9Si_2Fe_2$ phase [11]. For refinement and the morphology change to occur the UST had to be applied in the temperature range of peritectic reaction (585-597 °C [12]) L+δ-Al_4FeSi_2 → Si+β-phase +Si [13, 14].

Table 2. Chemical composition analysis of iron intermetallic without and with UST applied at across liquidus stage

Iron intermetallics phases	Elements (at.%)				Possible phase
	Al	Si	Fe	Fe/Si	
Needle plate-like (No UST)	63.8	18.9	17.3	0.92	β-$Al_9Si_2Fe_2$
Rod-like (UST)	72.6	14.1	13.3	0.94	β-$Al_9Si_2Fe_2$

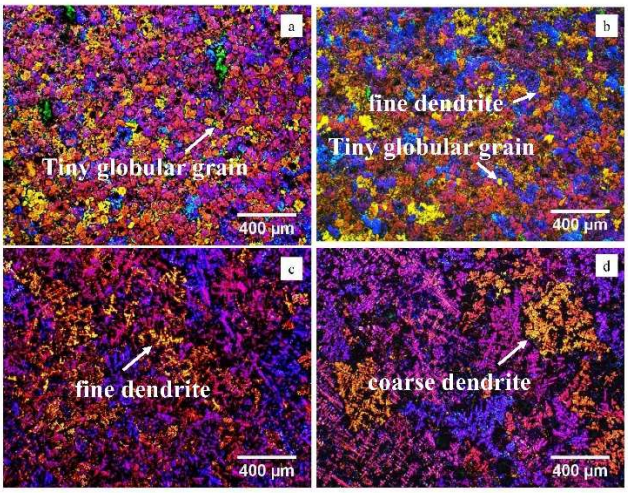

Figure 4. Optical micrographs illustrating the morphology and refinement of Al grains in the Al-Si piston alloy when UST was applied to: (a) mushy, (b) across liquidus, (c) liquid; and (d) No UST

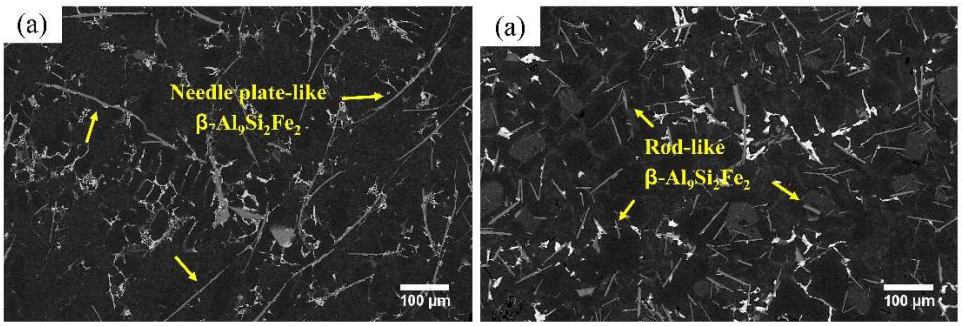

Figure 5. Microstructure showing the morphology of iron intermetallics in the Al-Si piston alloy: (a) without UST and (b) with UST at across the liquidus.

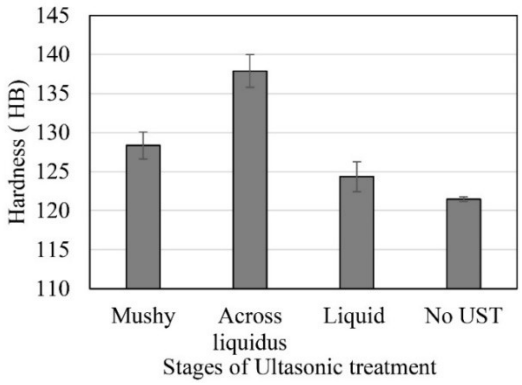

Figure 6. Hardness of the Al-Si piston alloy with high Cu content after UST applied at different stages of solidification.

3.3. Hardness measurements

In general, the hardness depends on the amount of hard particles and the size of Al grains. Figure 6 shows the effect of UST applied in different stages of solidification on the hardness of the high-Cu Al-Si piston alloy. In all cases the hardness of the alloys treated with ultrasound was higher than in the alloy solidified without UST. The largest gain in the hardness was achieved when UST was applied across the liquids (138 vs 122 HB). This correlates with the refinement of Al grains and increased amount of refined primary Si particles as well as finer intermetallics as can be seen in Figure 2f and Figure 4b. The alloy solidified without UST had coarser eutectic Si phases, large unevenly distributed primary Si and also large needle-like β particles, yet its hardness was the lowest, which gives indication of the significance of the size and distribution of hard particles for the overall alloy hardness.

4. Conclusions

- The refinement of primary Si particles can be achieved when the Al-Si piston alloy is treated by ultrasound in the liquid state (above liquidus).
- The application of UST during solidification (below liquidus and during eutectic reaction) refined Al grains through enhanced heterogeneous nucleation and dendrite fragmentation.
- The fragmentation mechanism is responsible for the modification of β-phase morphology from needle-like to rod-like structures, with simultaneous refinement of the particles.
- UST improves the hardness, particularly when UST is applied across the liquidus upon solidification.

Acknowledgements
This work was financially supported by The Research and Researchers for Industry (RRi) under the Thailand Research Fund (TRF) offers a scholarship for Ph.D. student (PHD57I0060) with Thai Metal Aluminium Co., Ltd and King Mongkut's University of Technology Thonburi through the "KMUTT 55th Anniversary Commemorative Fund". S.C. thanks BCAST (UK) for hosting a research visit.

References

[1] Y. Yang, K. Yu, Y. Li, D. Zhao, X. Liu, Evolution of nickel-rich phases in Al–Si–Cu–Ni–Mg piston alloys with different Cu additions, Materials & Design 33(1) (2012) 220-225.
[2] N. Belov, D. Eskin, N. Avxentieva, Constituent phase diagrams of the Al–Cu–Fe–Mg–Ni–Si system and their application to the analysis of aluminium piston alloys, Acta materialia 53(17) (2005) 4709-4722.
[3] S. Gencalp Irizalp, N. Saklakoglu, Effect of Fe-rich intermetallics on the microstructure and mechanical properties of thixoformed A380 aluminum alloy, Engineering Science and Technology, an International Journal 17(2) (2014) 58-62.
[4] G.I. Eskin, D.G. Eskin, Ultrasonic treatment of light alloy melts, CRC Press,2015.
[5] J.Y. Wang, B.J. Wang, L.F. Huang, Structural evolution of Al–8%Si hypoeutectic alloy by ultrasonic processing, Journal of Materials Science & Technology 33(11) (2017) 1235-1239.
[6] L. Zhang, D. Eskin, A. Miroux, L. Katgerman, Formation of microstructure in Al-Si alloys under ultrasonic melt treatment, Light Metals (2012) 999-1004.
[7] F. Wang, D. Eskin, T. Connolley, J.-w. Mi, Influence of ultrasonic treatment on the formation of primary Al3Zr in an Al-0.4 Zr alloy, (2017).
[8] F. Wang, D. Eskin, J. Mi, T. Connolley, I. Tzanakis, Refinement of Primary Al3Ti Intermetallic Particles in an Al-0.4 wt% Ti alloy by Ultrasonic Melt Processing.
[9] D.G. Eskin, Ultrasonic processing of molten and solidifying aluminium alloys: overview and outlook, Materials Science and Technology (2016) 1-10.
[10] F. Wang, D. Eskin, J. Mi, C. Wang, B. Koe, A. King, C. Reinhard, T. Connolley, A synchrotron X-radiography study of the fragmentation and refinement of primary intermetallic particles in an Al-35 Cu alloy induced by ultrasonic melt processing, Acta Materialia 141 (2017) 142-153.
[11] C.M. Dinnis, J.A. Taylor, A.K. Dahle, As-cast morphology of iron-intermetallics in Al–Si foundry alloys, Scripta Materialia 53(8) (2005) 955-958.
[12] L.-g. Hou, Y.-h. Cai, H. Cui, J.-s. Zhang, Microstructure evolution and phase transformation of traditional cast and spray-formed hypereutectic aluminium-silicon alloys induced by heat treatment, Int J Miner Metall Mater 17(3) (2010) 297-306.
[13] T. Maitra, S.P. Gupta, Intermetallic compound formation in Fe–Al–Si ternary system: Part II, Materials Characterization 49(4) (2002) 293-311.
[14] Y. Zhang, J. Jie, Y. Gao, Y. Lu, T. Li, Effects of ultrasonic treatment on the formation of iron-containing intermetallic compounds in Al-12%Si-2%Fe alloys, Intermetallics 42 (2013) 120-125.